Model of dynamic and macroscopic features of a floc blanket

D. H. Bache

ABSTRACT

Theory is developed to represent the macroscopic features of a floc blanket held in steady state. Flocs are treated as non-porous entities possessing a fractal structure. A particular feature of the analysis is the recognition of floc strength, floc sizes adjusting to the prevailing rate of energy dissipation within the blanket. Account is taken of the floc size distribution, with expressions derived to describe the blanket settling velocity and mass flux. Analysis of experimental data yielded detail of the blanket floc size scale (d_{vo}), water content and strength. The mass flux was maximised when the floc volume fraction was close to 0.17. It was shown that the upflow velocity (u) complied with the dependence $u \propto S_o/(Md_{max}^{5-D})$ in which d_{max} is a maximum floc size, M the blanket solids concentration, D the fractal dimension and S_o a strength scaling factor. Consideration was given to blanket characteristics in non-stationary conditions. The final section of the paper focuses on the attenuation capacity. It was argued that d_{vo} should be as low as practicable in order to promote the capture of feed flocs by interception, to reduce the water content of the solids waste stream when using hydrolysing coagulants, and may also enhance the mass flux.

Key words | attenuation, blanket, dynamics, floc, strength, upflow

D. H. Bache
Department of Civil Engineering,
University of Strathclyde,
Glasgow G4 0NG,
UK
E-mail: *d.bache@strath.ac.uk*

ABBREVIATIONS

A	cross-sectional area of blanket
A'	packing factor
c	suspended solids concentration
c_e	efflux suspended solids concentration
c_i	incoming suspended solids concentration
d	spherical equivalent diameter of floc
d_L	arithmetic mean value of d across length-size distribution
d_{max}	upper cut-off diameter in floc size distribution
d_o	reference particle size
d_{vo}	reference floc size tied to blanket permeability
d_{V95}	95th percentile in volume-size distribution
D	mass fractal dimension
E_c	collision efficiency
E_{adh}	adhesion efficiency
$f(\Phi_F)$	function tied to blanket permeability
g	gravitational acceleration
G	velocity gradient within blanket
k	fitting coefficient; Equation (4)
k	permeability; Equation (25)
K	a quasi-constant defined by Equation (22)
L	blanket thickness
L_0	blanket thickness at time $t = 0$; also used as minimum thickness after solids draw off
L_t	blanket thickness at time t
m_s	overall suspended solids mass within blanket
M	blanket suspended solids concentration
n_e	efflux floc number concentration
n_i	incoming floc number concentration
N	number concentration of flocs
p	fitting coefficient
Q	volumetric flow rate

doi: 10.2166/aqua.2010.029

r	fitting coefficient associated with $S_o^{'}$
S	floc strength
S_o	strength scale when $r = 1$
$S_o^{'}$	general strength scale
S_ϕ	distribution shape factor
t_L	liquid retention time
u	upflow velocity
U	size ratio ($= d/d_L$)
v_{sett}	blanket settling velocity
V_{floc}	overall floc volume within blanket
V_s	solids volume within V_{floc}
V_w	water volume within V_{floc}
α	trapping efficiency
β	attenuation coefficient
ΔP	pressure drop across blanket
ε	rate of energy dissipation per unit mass
$\bar{\varepsilon}$	spatial average value of ϵ ($= \nu G^2$)
λ_{max}	scaling ratio ($= d_{max}/d_L$)
λ_{vo}	scaling ratio ($= d_{vo}/d_L$)
μ	dynamic viscosity
ν	kinematic viscosity ($= \mu/\rho_w$)
ρ_e	density difference ($= \rho_f - \rho_w$)
ρ_f	floc density
ρ_s	density of floc solids
ρ_w	density of water
ϕ	solids volume fraction
Φ_F	floc volume fraction
$< \ldots >$	average value within specified volume or set

INTRODUCTION

The character and behaviour of the suspended bed within a floc blanket clarifier (FBC) lies at the heart of the process. The 'blanket' is held in place via a balance between the flux of material associated with the upflow and a downward solids flux associated with sedimentation. It consists of an assemblage of flocs whose sizes are relatively large compared with the incoming feed floc. The blanket acts as a filter of the incoming material–capture being controlled by both the rate of collision and the overall trapping efficiency. Material that is not captured, or breaks free from the blanket has direct impact on the load entering the filters.

Echoing developments of Ives (1968), Tambo & Hozumi (1979), Armirtharajah & O'Melia (1990) regarded the blanket as a turbulent reactor, with the efflux concentration of microflocs (n_e) defined by the relationship:

$$\frac{n_e}{n_i} = \exp\left(-\frac{\alpha G \Phi_F t_L}{\pi}\right) \tag{1}$$

In this expression, n_i refers to the number concentration of the microflocs entering the base of the blanket, α the trapping efficiency, G the velocity gradient, Φ_F the floc volume fraction, and t_L the liquid retention time.

As collection progresses, there is an accumulation of solids held within the suspended bed, this manifesting as an increase in the blanket thickness. Periodically, excess solids are bled off. Here the principal concern is with the bed dynamics in steady state conditions subject to the following constraints: (a) the solids mass held within the blanket remains constant, and (b) the blanket interface is sharp and (c) the blanket level is stationary. The latter assumption implies that

$$u = v_{sett} \tag{2}$$

in which u is the superficial velocity of loading ($= Q/A$), with Q as the volumetric flow and A, the cross-sectional area. Parameter v_{sett} refers to the rate of settlement defined by

$$v_{sett} = v_o f(\Phi_F) \tag{3}$$

where v_o is a scaling velocity and $f(\Phi_F)$ a function tied to the permeability of the suspended blanket. There exist many expressions for $f(\Phi_F)$, tending to be described by an empirical relationship of the form

$$f(\Phi_F) = (1 - k\Phi_F)^p \tag{4}$$

in which k and p (>0) are fitting coefficients and $0 < f(\Phi_F) \leq 1$.

In the analysis, a necessary task is to define the parameters Φ_F, G and t_L appearing in Equation (1), paying particular attention to the character of the floc. From this base, the principal objective is to gain a better understanding of how floc properties (particularly floc strength) are likely to affect the hydraulic and solids loading that can be sustained by the blanket. Ultimately, the upflow velocity is controlled by Equation (3); this looks deceptively simple,

until one recognises that Φ_F and perhaps also v_o are affected by u. Some progress was made on this theme in Bache & Gregory (2007). The analysis described in this paper provides a more accurate statement of the $\Phi_F(u)$ dependence and leads to a different view of how the product $G\Phi_F t_L$ is affected by u or $\Phi_F(u)$.

THEORY

Foundation framework

A blanket of depth L and uniform cross-sectional area (A) is assumed to be spatially homogeneous with respect to the solids concentration. The head loss or pressure drop (ΔP) across the blanket associated with the upflow, balances the pressure exerted by the buoyant weight of the floc, such that

$$\Delta P = L\Phi_F < \rho_e > g \tag{5}$$

where $< \rho_e >$ is the average density difference (ρ_f - ρ_w) within the blanket with $< \rho_f >$ as the average density of the flocs, ρ_w the density of water and g the gravitational acceleration. The liquid retention time is defined by

$$t_L = \frac{(1-\Phi_F)V}{Q} = \frac{(1-\Phi_F)L}{u} \tag{6}$$

in which V is the blanket volume. With this information, G is defined by

$$G = \left(\frac{\Delta P}{\mu t_L}\right)^{1/2} = \left(\frac{u\Phi_F g < \rho_e >}{(1-\Phi_F)\mu}\right)^{1/2} \tag{7}$$

The floc volume fraction can either be measured directly as described in Gregory *et al.* (1996) or deduced from the floc size distribution. An example of a distribution measured within a blanket using an underwater camera (noted in Bache *et al.* 2000) is shown in Figure 1. Sizes are expressed in the form d/d_L in which d is an equivalent diameter and d_L the arithmetic average value of d across the length-size distribution. Although the rising limb of the distribution is not evident (a symptom of the camera resolution), the distribution is unimodal and can be modelled using the framework described in Bache & Rasool (2006).

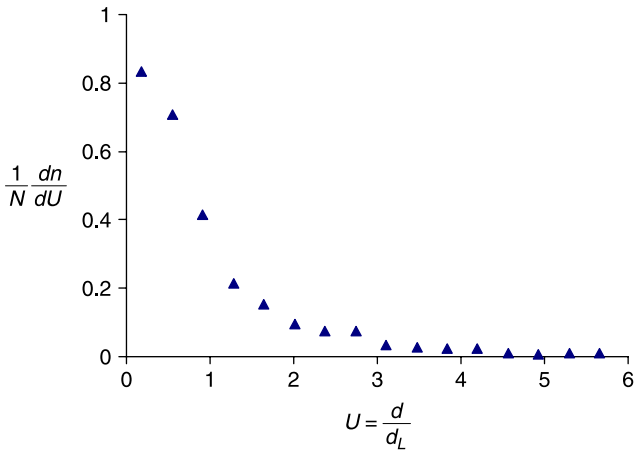

Figure 1 | Example of floc size distribution from a clarifier receiving a low turbidity coloured water coagulated with alum. N refers to the total number of flocs per unit volume, and δn is the number concentration in the interval U to $U + \delta U$.

Flocs have a fractal structure, implying that their critical properties scale with size. For example, the average solids concentration within an individual floc can be represented by

$$c = \rho_s A' \left(\frac{d}{d_o}\right)^{D-3} \tag{8}$$

in which ρ_s is the solids density, A' is a packing factor and d_o a scaling length representative of the diameter of the particles from which the floc is formed. D is the mass fractal dimension in which $1 \le D \le 3$. The value $D = 1$ corresponds to particles joined together in a chain form or necklace-type structure whereas $D = 3$ corresponds to a uniform solid continuum in a spherical object. By summing the volume of the flocs across the distribution and recognising that each floc carries mass (such as represented by Equation (8)), Bache & Rasool (2006) showed that the floc volume fraction could be expressed by

$$\Phi_F = \frac{M}{\rho_s A'} \left(\frac{d_L}{d_o}\right)^{3-D} S_\phi(D) \tag{9}$$

in which M is the mass concentration (suspended solids mass per unit volume) and S_ϕ (D) is a distribution shape factor that combines information about the shape of the volume-size distribution and the mass-size distribution. (NB Equation (9) has been corrected for a typographic

error in the original). When applied to a floc blanket, it should be recognised that M is expressed by the identity:

$$M = \frac{m_s}{LA} \tag{10}$$

where m_s refers to the suspended solids mass held within the blanket. The average solids concentration $< c >$ across the total floc volume ($V_{floc} = \Phi_F LA$) is:

$$< c >= \frac{m_s}{V_{floc}} = \frac{M}{\Phi_F} \tag{11}$$

This can be translated to the average density difference (appearing in Equation (5)) using the transformation

$$c = \frac{\rho_e}{1 - \rho_w/\rho_s} \tag{12}$$

leading to

$$< \rho_e >= \frac{m_s}{LA\Phi_F}\left(1 - \frac{\rho_w}{\rho_s}\right) \tag{13}$$

The next stage is to gain insight into the size ratio (d_L/d_o). In stirred suspensions, this generally depends on the size of the largest flocs (d_{max}) within the distribution, and on the distribution shape. For convenience, one may write

$$d_{max} = \lambda_{max} d_L \tag{14}$$

When a distribution has a universal shape, the scaling ratio (λ_{max}) defined by Equation (14) remains constant in response to the external factors that alter d_L; this applies to any size scale representing characteristic features of the size distribution (see Bache & Rasool 2006). Referring to the distribution shown in Figure 1, $d_L = 580\,\mu m$ and the largest sizes are *c*. 4,400 μm (corresponding to d_{V95}, the 95th percentile in the volume size distribution). Hence $\lambda_{max} \approx 7.6$ for the distribution shown. The reason that one focuses on the largest flocs is that these are the weakest (and thus most vulnerable to the prevailing hydrodynamic forces). Sonntag & Russel (1987) argued that floc strength (S) was likely to be of the form

$$S = S_o'\left(\frac{d}{d_o}\right)^{r(D-3)} \tag{15}$$

in which S_o' is a strength scale and r (≥ 1) is a coefficient reflecting the sensitivity of strength to the floc's internal solids volume concentration. From a balance of floc strength and available turbulence kinetic energy per unit volume, Bache (2004) showed that

$$\frac{d_{max}}{d_o} = \left(\frac{30 S_o' \nu}{\rho_w d_o^2 \varepsilon}\right)^{\frac{1}{2+r(3-D)}} \tag{16}$$

where ν is the kinematic viscosity and ε the local rate of energy dissipation per unit mass.

Equation (16) applies to the viscous domain. To simplify the analysis, it will be assumed that $r = 1$ (likely to apply to flocs with a relatively open network of linear structures; see Bache 2004). In this case, S_o' has the particular identity S_o (see Bache 2004) in which $S_o \propto A'$. Again to simplify analysis, it is assumed that $\epsilon = \bar{\varepsilon}$, where $\bar{\varepsilon}$ refers to the spatial average value of ϵ within the blanket, allowing one to write

$$\bar{\varepsilon} = \nu G^2 \tag{17}$$

With these simplifications, Equation (16) reduces to

$$\frac{d_{max}}{d_o} = \left(\frac{30 S_o}{\rho_w d_o^2 G^2}\right)^{\frac{1}{5-D}} \tag{18}$$

Combination of Equations (9), (10), (14), (15) and (18) leads to

$$\Phi_F = \frac{m_s}{LA\rho_s A'}\left(\frac{30 S_o}{\rho_w d_o^2 G^2}\right)^{\frac{3-D}{5-D}} \frac{1}{\lambda_{max}^{3-D}} S_\phi(D) \tag{19}$$

The next step is to discern how the blanket responds to changes in u as a quasi-independent variable. Increases in u cause the blanket to expand, thereby causing a reduction in Φ_F. Making use of Equation (13), Equation (7) becomes

$$G = \left[\frac{g m_s u}{\mu AL(1 - \Phi_F)}\left(1 - \frac{\rho_w}{\rho_s}\right)\right]^{1/2} \tag{20}$$

With this definition, Equation (19) can be cast in the form

$$L\Phi_F = K\left(\frac{(1 - \Phi_F)L}{u}\right)^{\frac{3-D}{5-D}} \tag{21}$$

with

$$K = \frac{m_s}{A\rho_s A'}\left(\frac{30S_o\mu A\rho_s}{g\rho_w d_o^2 m_s(\rho_s-\rho_w)}\right)^{\frac{3-D}{5-D}}\frac{1}{\lambda_{max}^{3-D}}S_\phi(D) \quad (22)$$

K can be regarded as a constant when the parameters on which it depends (particularly m_s) remain at fixed values. With knowledge of D, an estimate of K and the observed variation $L(u)$, Equation (22) can be solved numerically to yield the $\Phi_F(u,K)$ dependence. The principal response to velocity is described by:

$$\Phi_F = \frac{1}{1+u(L\Phi_F)^{2/(3-D)}/K^{(5-D)/(3-D)}} \quad (23)$$

in which the product $L\Phi_F$ is weakly varying, reflecting potential changes in the floc volume as a result of changes in G.

The solution of Equation (21) is necessarily constrained by the condition $u = v_{sett}$ as expressed by Equation (2). This demands knowledge of both v_o and $f(\Phi_F)$. Ideally, the form of v_{sett} should be determined experimentally with behavioural features cast in terms of Equations (3) and (4) or their equivalent. In the absence of such information, the magnitude of v_{sett} can be estimated using the framework described below.

In viscous flows, it may be shown (e.g. Gmachowski 2002) that the settling velocity of an assemblage of spheres of solids fraction ϕ is expressed by

$$v_{sett} = \frac{\phi(\rho_s-\rho_w)g}{\mu}k \quad (24)$$

where k is the permeability of the assemblage and μ the dynamic viscosity. Probstein 1994, p. 269) cites a Happel model for uniform spheres in which k is specified by the identity

$$k = \frac{1-(3/2)\phi^{1/3}+(3/2)\phi^{5/3}-\phi^2}{18\phi[1+(2/3)\phi^{5/3}]}d^2 \quad (25)$$

Substitution into Equation (24), and making use of Equation (3), leads to the well-known Stokes expression

$$v_o = \frac{gd^2(\rho_s-\rho_w)}{18\mu} \quad (26)$$

together with $f(\phi)$ defined by

$$f(\phi) = \frac{1-(3/2)\phi^{1/3}+(3/2)\phi^{5/3}-\phi^2}{1+(2/3)\phi^{5/3}} \quad (27)$$

Equations (26) and (27) can be adapted for use with flocs by adopting the identity $\phi \equiv \Phi_F$ when flocs are non-porous. Because Equation (24) is a macroscopic model of the assemblage, the density difference must also be a macroscopic parameter with $<\rho_e>$ defined by Equation (13). With this information, Equation (26) becomes

$$v_o = \frac{m_s}{\Phi_F LA}\left(1-\frac{\rho_w}{\rho_s}\right)\frac{gd_{vo}^2}{18\mu} \quad (28)$$

in which d_{vo} is a reference size tied to the permeability of the assemblage. Replacing $\Phi_F L$ using Equation (9) leads to

$$v_o = \frac{gA'(\rho_s-\rho_w)d_o^2}{18\mu S_\phi(D)}\cdot\frac{\lambda_{vo}^2}{\lambda_{max}^{D-1}}\left(\frac{d_{max}}{d_o}\right)^{D-1} \quad (29)$$

In Equation (29), parameter λ_{vo} is defined by $d_{vo} = \lambda_{vo}d_L$, this being interpreted in the same way as Equation (14) with respect to d_{max}. Making use of Equation (18), Equation (29) may also be stated as

$$v_o = \frac{gA'(\rho_s-\rho_w)d_o^2}{18\mu S_\phi(D)}\cdot\frac{\lambda_{vo}^2}{\lambda_{max}^{D-1}}\left(\frac{30S_o}{\rho_w d_o^2 G^2}\right)^{\frac{D-1}{5-D}} \quad (30)$$

This shows the explicit dependence of v_o on the strength scale.

APPLICATION OF THEORY

Su *et al.* (2004) described the behaviour of a blanket formed from a suspension of clay coagulated with PACl. Following coagulation, sediment was collected and carefully transferred to cylindrical column of 5.5 cm diameter, through which clean water was pumped; this allowed a fluidised bed to be established. Figure 2 shows the response of the blanket height to upflow velocity at three doses of PACl. The plots correspond to steady state tests, the trends also displaying effluent turbidity values. From detail of experiments carried out at the optimum dose, it appears the solids mass (m_s) within the blanket was 3,537 mg. For illustrative purposes,

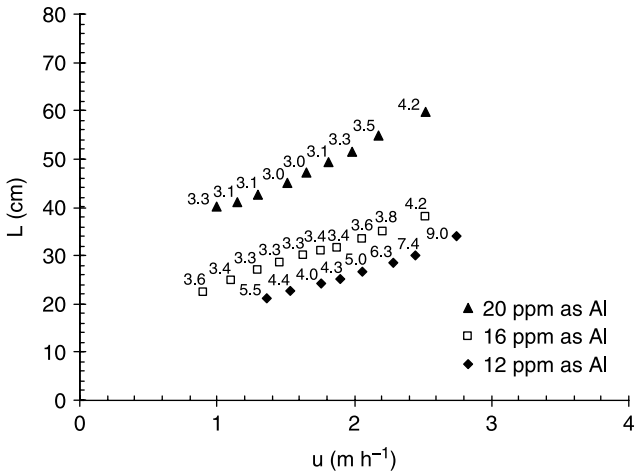

Figure 2 | Equilibrium heights and effluent turbidities of coagulated suspensions in response to the upflow velocity (Su *et al.* 2004).

it is assumed that the clay has the same characteristics as kaolin with $\rho_s \approx 2{,}600\,\mathrm{kg\,m^{-3}}$ and $d_o \approx 3.5\,\mu\mathrm{m}$. From studies of flocs of this type, Tambo & Watanabe (1979) found that the size-density relationship (Equation (31)) was sensitive to the 'ALT ratio'. This describes the ratio of the Al dose ($\mathrm{mg\,l^{-1}}$) to the suspended solids of the suspension ($1{,}600\,\mathrm{mg\,l^{-1}}$ in the study by Su *et al.* 2004). Thus at the optimum dose (16 mg Al/l), ALT = 16/1600 = 1:100 or 0.01. Data from Tambo & Watanabe (1979) were represented by the fractal dependence

$$\rho_e = A'(\rho_s - \rho_w)\left(\frac{d}{d_o}\right)^{D-3} \tag{31}$$

(arising from the combination of Equations (8) and (12)) which yielded plots of $A'$and D as a function of the ALT value (in Bache & Gregory (2007) as Figure 3.12); the latter indicates $A' \approx 5$ and $D \approx 1.9$ when ALT ≈ 0.01. With this information one can progress with the analysis of the data shown in Figure 2.

Optimisation procedure

By adopting trial values of K, $\Phi_F(K)$ may be calculated using Equation (21) for each pair of L, u values; this allows $f(\Phi_F(K))$ to be deduced using Equation (27). From this one can determine $v_o(K) = u/f(\Phi_F(K))$. In principle, this yields an estimate of $d_{vo}(K)$ using Equation (28). Thereafter optimisation depends on the following logic:

$$d_{vo} \propto \left[\frac{u\Phi_F L}{f(\Phi_F)}\right]^{1/2} \tag{32}$$

and

$$\Phi_F L \propto d_{max}^{3-D} \tag{33}$$

Linearity between d_{vo} and d_{max} requires that

$$\frac{u}{f(\Phi_F(K))} \propto [\Phi_F(K)L]^{(D-1)/(3-D)} \tag{34}$$

By testing this condition across the set, K can be optimised for each set of $u - L$ pairs; this yielded optimised values of Φ_F, v_o and d_{vo}. The outcome of the analysis is summarised in Table 1.

DISCUSSION

Data and model integrity

Data in Table 1 provides detail of the way in which the parameters respond to changes in u. The particular solution rests heavily on the choice of $f(\Phi_F)$. Here, it is not claimed that Equation (27) represents the character of the suspension used. Rather, it permits one to demonstrate the viability of the analysis. At the outcome, it was

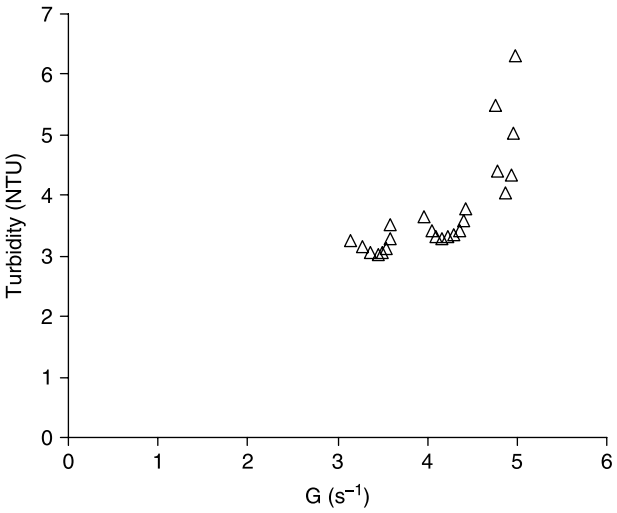

Figure 3 | Association between effluent turbidity values shown in Figure 2 and *G*.

Table 1 | Estimates of optimised parameters associated with trends shown in Figure 2 based on solution of Equation (21)

u (m h^{-1})	L (cm)	Φ_F	$f(\Phi_F)$	$L\Phi_F$ (cm)	v_o (m h^{-1})	d_{vo} (μm)	G (s^{-1})	t_L (s)	$G\Phi_F t_L$
12 ppm	*($K = 2.895$)*								
1.36	21.2	0.316	0.090	6.79	15.2	780	4.72	383	571
1.53	22.7	0.293	0.103	6.66	14.9	771	4.76	377	527
1.76	24.3	0.270	0.118	6.57	15.0	767	4.85	363	476
1.89	25.2	0.259	0.126	6.52	15.0	766	4.90	355	451
2.06	26.6	0.244	0.137	6.50	15.0	763	4.92	353	424
2.28	28.5	0.227	0.152	6.48	15.1	763	4.95	348	391
2.45	30.1	0.215	0.163	6.48	15.1	763	4.95	348	371
2.78	34.1	0.192	0.185	6.56	14.8	762	4.86	361	338
16 ppm	*($K = 3.443$)*								
0.90	22.5	0.400	0.053	9.00	17.0	957	3.94	540	850
1.11	24.8	0.357	0.069	8.86	16.0	920	4.02	517	743
1.30	27.0	0.325	0.085	8.78	15.4	898	4.07	504	668
1.45	28.4	0.306	0.095	8.69	15.2	890	4.14	489	619
1.63	30.0	0.286	0.107	8.59	15.2	884	4.21	473	569
1.76	30.9	0.275	0.115	8.49	15.4	883	4.27	458	538
1.88	31.7	0.265	0.121	8.41	15.5	883	4.33	446	512
2.06	33.4	0.250	0.133	8.35	15.6	881	4.37	438	479
2.21	34.9	0.238	0.142	8.32	15.6	880	4.40	433	454
2.51	37.8	0.218	0.159	8.26	15.8	882	4.44	424	411
20 ppm	*($K = 5.364$)*								
0.99	40.0	0.412	0.049	16.5	20.3	1,415	3.13	854	1,102
1.14	41.1	0.390	0.056	16.0	20.3	1,396	3.26	788	1,002
1.30	42.5	0.370	0.064	15.7	20.2	1,376	3.35	743	922
1.51	45.1	0.342	0.076	15.4	19.8	1,351	3.44	705	831
1.65	47.1	0.325	0.085	15.3	19.5	1,336	3.47	695	784
1.81	49.4	0.308	0.094	15.2	19.3	1,323	3.51	679	733
1.98	51.5	0.292	0.103	15.1	19.2	1,316	3.56	662	689
2.18	54.8	0.274	0.115	15.0	19.0	1,305	3.57	657	643
2.52	59.6	0.250	0.133	14.9	19.0	1,299	3.62	638	577

by no means certain whether the framework would lead to an optimised solution. It did. In each set, it is seen that G tends to increase with u, with the consequence that the reference size (d_{vo}) is reduced. Although there are changes in v_o as a result of changes in size, the principal means by which the balance $u = v_{sett}$ is achieved is by changes in Φ_F, thereby altering $f(\Phi_F)$. Generally it is seen that the changes in G, d_{vo} and v_o are relatively small, but are nevertheless vital to the dynamics of the system.

Although the efficacy of the analytical scheme has been demonstrated, it is not clear whether the solution is physically realistic. This can be judged in a number of ways. The least satisfactory (but nevertheless of interest) is the behaviour of the turbidity values marked on the plots in Figure 2. Generally these have similar values within each data set when $u < 2\,\mathrm{m\,h^{-1}}$ and increase at larger u values. There are a number of factors that may give rise to the turbidity behaviour. For example, when G increases and floc sizes become reduced, the turbidity might

emanate from unattached debris associated with the rupture process. Closely related, is the possibility that turbidity is generated by surface erosion, shear forces being scaled by μG. Turbidity values will also increase when small flocs break away from the blanket because their settling velocity is too small. At this condition, the interface becomes diffuse, reflecting non-uniformity in the solids concentration (see Figure 3 in Su *et al.* (2004) together with photographic evidence in Sung *et al.* (2005). It is likely that some of the highest values of turbidity shown in Figure 2 may be associated with the approach to the critical state ($u > v_{sett}$) at which hindered settlement breaks down and a blanket cannot exist. If one neglects these higher values, there is a weak correlation between the average turbidity and the average G value for each set as shown in Figure 3.

A second means of judging the outcome of the analysis is to examine the average floc water content associated with each dose. This aspect is summarised in Table 2. The average floc volume is estimated as $A < L\Phi_F >$ where $< \ldots >$ denotes an average across each set shown in Table 1. Within this, the solids volume ($V_s = m_s/\rho_s$) is small. Column 6 shows the relationship between the water amount (V_w) and the dose, the ratio being of similar magnitude. This aspect has several messages. Aside from the impact of upflow, the analysis suggests that water content is a major factor affecting the separation of the trends shown in Figure 2. Second, the association between dose and water content is roughly in line with expectation for the following reason. At the pH used in the study (pH 7), the structure of PACl is likely to break down as a result of hydrolysis, leading to the production of a bulk precipitate (see Furrer *et al.* 1992 concerning the behaviour of Al_{13} (a component of PACl), together with data from Van Benschoten & Edzwald 1990 concerning PACl, which is plotted in Figure 1.30 of Bache & Gregory 2007). The bulk precipitate is water binding–an attribute that is scaled by the amount of precipitate present and dose dependent.

Table 2 | Impact of the dose on water content and strength scale

Al dose (ppm)	$<L\Phi_F>$ (cm)	V_{floc} (ml)	V_s (ml)	V_w (ml)	V_w/Dose (ml/ppm)	S_o (N m^{-2})
12	6.56	167.4	1.4	166	13.8	0.17
16	8.57	218.9	1.4	217	13.6	0.21
20	15.46	394.5	1.4	393	19.7	0.50

Column 7 shows estimates of S_o, these also being dependent on the dose. The largest value of S_o occurs at the highest dose. It is this facet (through its control on floc size) which is ultimately responsible for the capacity of the floc to retain water. The particular values cited are in the range reported in Bache (2004) for Al-Kaolin flocs (0.1–0.5 N m^{-2}). The similarity of these values is rather surprising, given the vastly different regimes for estimating their values. It may imply that $d_{vo} \approx d_{max}$ for the suspension under study.

Overall, the analysis appears to lead to deductions which are physically reasonable.

Towards practice

When it comes to practice, there are a host of questions and issues. For example, is there an optimum u value? How does one integrate the concepts described in this paper with the workings of an FBC? Here, some foundation issues are addressed in the context of the data from Su *et al.* (2004).

Mass flux

On the basis of pilot plant testing, Gregory (1979) suggested that the optimum load might be guided by the maximum solids flux condition within the blanket–this being represented by the product Mv_{sett}. Combination of Equations (3), (10) and (28) shows

$$Mv_{sett} = \left(\frac{m_s}{L\Phi_F A}\right)^2 \left(1 - \frac{\rho_w}{\rho_s}\right) \frac{g d_{vo}^2}{18\mu} \Phi_F f(\Phi_F) \tag{35}$$

Following a series of substitutions and manipulation, this takes the form

$$Mv_{sett} = \left[\frac{\rho_s A' d_o \lambda_{vo}}{S_\phi(D)\lambda_{max}^{D-2}}\right]^2 \frac{g}{18\mu} \left(\frac{d_{max}}{d_o}\right)^{2D-4} \Phi_F f(\Phi_F) \tag{36}$$

When $f(\Phi_F)$ is defined by Equation (27), the product $\Phi_F f(\Phi_F)$ has a maximum at $\Phi_F = 0.172$. Figure 4 shows the mass flux trends associated with the data shown in

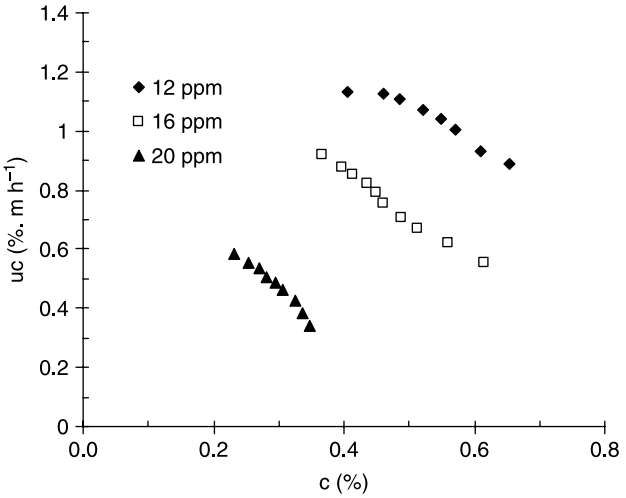

Figure 4 | Trends in the solids flux based on data shown in Figure 2.

Table 1–the highest flux values being associated with the 12 ppm set. In the case of this trend, one can see evidence of the approach to a maximum at $c(\%) \approx 0.4$. From data in Table 1, it is evident that this condition is associated with the highest upflow at which $\Phi_F = 0.192$–this being close to the critical value (0.172) noted above.

In order to gain insight into the factor(s) responsible for this mode of behaviour, a sensitivity analysis was carried out on the basis of both Equations (35) and (36). In the case of Equation (36) (treating $d_{max} \equiv d_{vo}$), the index value (2D-4 ≈ -0.2) nullifies the direct impact of floc size and $\Phi_F f(\Phi_F)$ has similar values across the sets. From this, differences in mass flux must be attributed to parameters contained in the term $[\ldots]^2$. In contrast, Equation (35) provides a direct account of the behaviour. Within Equation (35), it is recognised that $m_s/L\Phi_F A \equiv <c>$ refers to the average solids concentration within the floc. When flocs have a greater water content, they will tend to be bigger and $<c>$ will be relatively low, whereas the opposite occurs when flocs have a lower water content. Equation (35) shows that the impact of the $<c>$ term is offset by the magnitude of d_{vo}–the flux being controlled by the behaviour of the product $<c> d_{vo}$. In the context of Figure (4), it is the $<c>$ term which dominates–the largest mass flux occurring in the 12 ppm set, in which the flocs have a lower water content and are smaller (supporting data in Tables 1 and 2).

The upshot of the analysis is that the maximum flux condition is not necessarily favoured by the strongest or largest flocs. In the case of the data shown in Figure 4, the maximum flux condition is favoured by the dose at which the floc volume is lowest.

Blanket floc strength

Gregory (1979) examined the impact of dosing polyelectrolytes for floc strengthening on the blanket solids concentration and on the renovation capacity under conditions in which the raw water quality, coagulant dose and upflow velocity were all held constant. In the case of the latter, it was shown that M increased according to dose or effectiveness of the polyelectrolyte. It was also found that the renovation capacity approached a limiting value as increasing amounts of polyelectrolyte were added, leading Gregory *et al.* (1999) to suggest there was little point in applying polyelectrolyte (or increasing the dose) if the blanket floc volume concentration is greater than about 18%.

Focusing on the first of these issues, if u is constant and one assumes that the blanket level was maintained at a fixed value, it implies that $v_o f(\Phi_F) = u$ remains constant for the conditions described. Because one would expect floc sizes to increase with the polymer dose (as a result of increased strength), this will manifest as an increase in v_o, implying that $f(\Phi_F)$ must decrease in order to maintain v_{sett} at the same value; hence Φ_F must increase with increasing dose. This can be demonstrated more formally using Equation (30), whereby the condition can be stated as

$$\frac{gA'(\rho_s - \rho_w)d_o^2}{18\mu S_\phi(D)} \cdot \frac{\lambda_{vo}^2}{\lambda_{max}^{D-1}} \left(\frac{30S_o}{\rho_w d_o^2 G^2}\right)^{\frac{D-1}{5-D}} f(\Phi_F) = \text{constant} \qquad (37)$$

To illustrate the implications of altering the strength scale, it will be assumed that D remains constant and (for simplicity) potential changes in the distribution shape as a result of strength are ignored. In these circumstances, Equation (37) is steered by the grouping

$$A'\left(\frac{S_o}{G^2}\right)^{\frac{D-1}{5-D}} f(\Phi_F) = \text{constant} \qquad (38)$$

When the depth of the blanket and u are fixed, Equations (10) and (20) combine to show

$$G \propto \left[\frac{M}{(1-\Phi_F)}\right]^{1/2} \tag{39}$$

Hence Equation (38) can be restated as

$$A'\left(\frac{S_o(1-\Phi_F)}{M}\right)^{\frac{D-1}{5-D}} f(\Phi_F) = \text{constant} \tag{40}$$

A schematic calculation to illustrate the implications of Equation (40) is based on the data shown in Table 3. Floc data (S_o, A', D) are taken from Bache & Rasool (2006) and refers to aluminium-kaolin flocs. The solids concentration data (M) is taken from Figure 10 of Gregory (1979), the source water being a lowland river. The value $\Phi_F = 0.18$ is an assumed value when strengthening agents were present. With this information, and using Equation (27) to estimate $f(\Phi_F)$, the constant on the right hand side of Equation (40) can be evaluated when a polymer is present. Making use of this value, the magnitude of Φ_F (= 0.05) was deduced using the associated data.

The example indicates that Φ_F changes in the same sense as M (as one would anticipate from Equation (9)). Thus, for the particular example, the theoretical explanation appears to be plausible.

One can also examine the association between strength and upflow using Equations (18) in combination with Equation (7), these showing

$$\frac{uM}{S_o(1-\Phi_F)}\left(\frac{d_{max}}{d_o}\right)^{5-D} = \frac{30\mu}{\rho_w d_o^2 g(1-\rho_w/\rho_s)} \tag{41}$$

In essence, the terms on the right hand side of Equation (41) are quasi-constants, whereas those on the left hand side are more variable. If the mass flux is maximised, the term $(1-\Phi_F)$ can be regarded as quasi-constant (≈ 1 for typical values of Φ_F encountered in practice). Ignoring this term shows $u \propto S_o/Md_{max}^{5-D}$. This highlights the explicit dependence of u on S_o. Further, when u is constant and S_o is increased by polymer addition (such as described above), one sees that increases in strength must be offset by increases in the product Md_{max}^{5-D}. At this point in time, it is not feasible to distinguish between the dependences on M and size. One way or the other, it appears that Φ_F will increase as a result of polymer addition–this improving the potential renovation capacity. However, in later analysis it will be shown that the blanket floc size (as well as Φ_F) plays a critical role in the trapping capacity–a facet which may be linked to the tailing off of the renovation capacity noted above when the polymer dose is increased as reported above. Experience also shows that, with increasing polymer dose, the floc becomes too sticky–manifesting as an inability to flow out of the sludge hoppers.

Table 3 | Data for inclusion in Equation (40)

	A'	D	S_o (N m^{-2})	M (g l^{-1})	Φ_F	$(1-\Phi_F)^{0.30} f(\Phi_F)$
No polymer	3.32	1.93	0.09	0.4	0.05	0.447
Polymer	3.32	1.93	7.1	1.8	0.18	0.188

Time-varying conditions

When one considers the analytical framework in the context of an operating plant, account must be taken of the solids content in the feed flow. As material gets trapped in the blanket, its solids content (m_s) will increase; this manifesting as an increase in the blanket height. This will continue until solids are bled off. Here, it is necessary to examine the likely impact of the added mass on the dynamics as described previously. This can be addressed at two levels, the superficial explanation being more straightforward. The theoretical framework described above is tied to the behaviour of an assemblage of particles whose flow characteristics are described by Equations (24) – (27). Adding particles of similar kind should not alter the dynamics provided ϕ or Φ_F remain constant. Readers wishing to probe this question at a deeper level are referred to Probstein (1994, pp. 267 – 269) in which the dynamics within a 'Happel cell' are related to the dynamics of the assemblage. When u and Φ_F remain at fixed values, Equation (21) shows that $L \propto m_s$; that is, M (defined by Equation (10)) maintains a fixed value. Thus:

$$\frac{dL}{dt} = \frac{1}{AM}\frac{dm_s}{dt} \tag{42}$$

Equation (20) shows that G remains constant when $L \propto m_s$, whereas t_L (defined by Equation (6)) increases as a result of the increase in L. Hence the only parameter within

the product $G\Phi_F t_L$ that responds to mass accumulation is the timescale (*provided* M and Φ_F remain constant). With these background factors in place, the following illustrates how the various strands of the analysis can be brought together into a dynamic model.

Mass conservation across a blanket in which there is both an inflow and an outflow is represented by the statement

$$\frac{dm_s}{dt} = Qc_i - Qc_e \tag{43}$$

where c_i and c_e refer to the incoming solids concentration and the outgoing solids concentration, respectively. Note that c_i and c_e are proportional to n_i and n_e appearing in Equation (1). Thereafter Equation (43) with the aid of Equations (1), (6) and (10) leads to the expression

$$\frac{dL}{dt} = \frac{uc_i}{M}[1 - \exp(-\beta L)], \tag{44}$$

with

$$\beta = \frac{\alpha G\Phi_F(1-\Phi_F)}{\pi u} \tag{45}$$

Making use of the boundary conditions, $L = L_0$ at $t = 0$ and $L = L_t$ at time t, integration of Equation (44) yields

$$L_t - L_0 + \frac{1}{\beta}\ln\left(\frac{1-\beta\exp(-\beta L_t)}{1-\beta\exp(-\beta L_0)}\right) = \frac{uc_i t}{M} \tag{46}$$

This can be solved numerically to show the change in blanket level with time. In the particular case of no losses ($\beta = 0$), $L_t - L_0 = uc_i t/M$. With knowledge of L_t, the quality of the outgoing stream is expressed by

$$c_e(t) = c_i \exp\left[-\frac{\alpha G\Phi_F(1-\Phi_F)L_t}{\pi u}\right] \tag{47}$$

Aside from the impact of other parameters, a worst case condition exists when the blanket is at its minimum height (say L_0) where L_0 might refer to the state of the blanket after solids withdrawal.

Trapping behaviour

At this point it is instructive to examine the impact of α on clarification. When the feed particles/flocs are larger than a few μm (eliminating the effects of Brownian motion) and when the density of the incident particles is close to the suspending fluid (eliminating the effects of inertia), trapping by the collector particles/flocs is dominated by interception. Feed particles will tend to follow the streamlines round the collector particles. Collection can only take place if they lie within the 'collision cross-section'. The boundary of the collision cross-section is determined by the trajectory of the incident particle which passes sufficiently close to the collector to enable attractive van de Waals forces to pull the incident particle towards the surface. This tendency of bond formation/adhesion will be offset by the effect of surface shear which acts to break such bonds and a hydrodynamic interaction arising from the displacement of fluid as the incident particle approaches the collecting surface. So collection depends on an appropriate trajectory together with the impact of a variety of forces acting on the incident particle/floc as it approaches the collection surface. In simplified models (e.g. Tambo & Hozumi 1979), these effects are separated into two processes with α defined by $E_c E_{adh}$ where E_c refers to the collision efficiency (based on a limiting trajectory in the absence of surface force fields) and E_{adh} the adhesion efficiency. In more refined models (e.g. Spielman 1977), the definition of the limiting trajectory includes the effect of the force fields and is more rigorous. However, flocs morphology is such that they differ from the ideal spherical particles considered in theory, so existing theory has only limited value in the task of defining α. The best way of determining its value is via the observed attenuation behaviour, coupled with knowledge of the remaining parameters featured in Equation (47).

Figure 5 illustrates the relative impact of the terms α and $G\Phi_F(1-\Phi_F)L_0$ on attenuation. Calculations were based on G, Φ_F, u data shown in Table 2 at a fixed depth ($L_0 = 0.6$ m). Figure 5(a) is based on the fixed value $\alpha = E_c = 0.004$ for inclusion in Equation (47); that is, deliberately ignoring the potential impacts of particle size, but displaying some attenuation. At each dose, the overflow water quality deteriorates with increasing u, the dose appearing to have relatively little impact on c_e/c_i because of the similarity of the $G\Phi_F(1-\Phi_F)L_0$ values at the same upflow velocity. In contrast, Figure 5(b) shows the potential impact of floc size scale (d_{vo}) within the blanket when the feed flocs have a

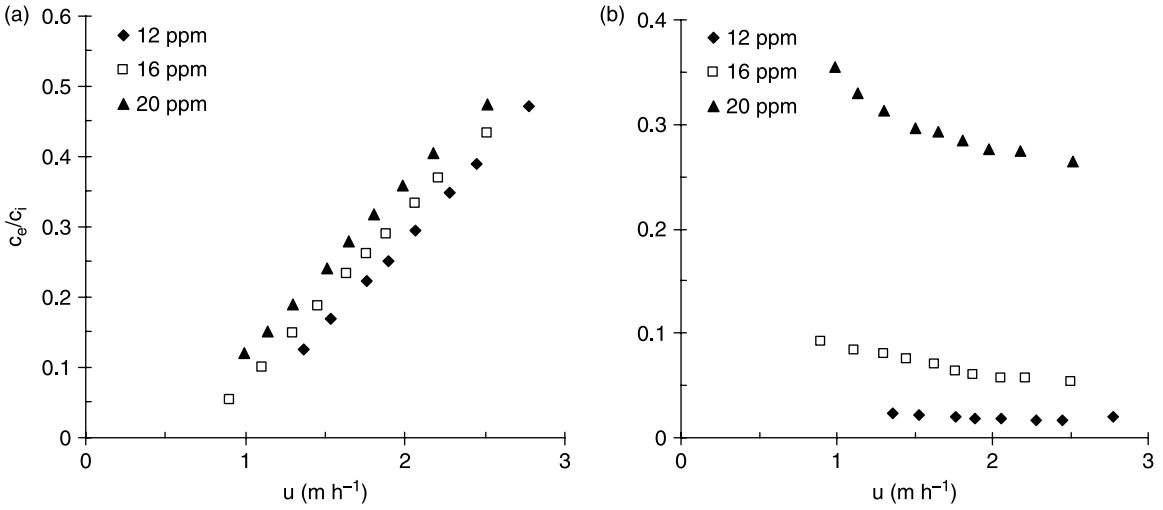

Figure 5 | (a) capture ratio at $\alpha = 0.004$ revealing sensitivity to $G\Phi_F$ $(1 - \Phi_F)$ L/u and (b) illustrating potential impact of floc sizes when α is defined by Equation (48) with $d_p = 40\,\mu m$.

size scale (d_p) of 40 μm, with E_c defined by

$$E_c = \frac{3}{2}\left(\frac{d_p}{d_{vo}}\right)^2 \tag{48}$$

Equation (48) refers to the collection efficiency of neutrally buoyant spherical particles in viscous flow conditions when surface interactions are excluded (e.g. Probstein 1994). A comparison between Figure 5(a) and (b) indicates that the inclusion of particle size impacts transforms the blanket attenuation capacity, best collection being favoured by conditions in which the ratio d_p/d_{vo} is at its largest (i.e. when d_{vo} has its smallest values); this occurs at the lowest dose and at the highest values of upflow. However, the response to upflow depicted in Figure 5(b) is unrealistic, because experience shows that the clarified water quality tends to diminish with increasing upflow (see Gregory *et al.* 1999). The reason is that Equation (48) overstates the collection efficiency. Tambo & Hozumi (1979) attempted to examine the effect of feed floc size on the attenuation capacity. When the feed floc sizes were larger, there was some improvement in the overflow water quality, but the effects were relatively small (possibly because the blanket floc sizes also changed). Although the trends in Figure 5(b) overstate the impact of floc size, they emphasise that losses in the value of $G\Phi_F(1 - \Phi_F)$ as u increases (as shown in Figure 5(a)) can be offset by improvements in the trapping efficiency by virtue of reductions in the blanket floc size scale. Here it should be emphasised that parameter d_{vo} merely reflects a size scale. In practice, collection will be greatly influenced by the spread of floc sizes, particularly the smaller sizes; these occur in greater number concentration (see Figure 1) and also offer a more favourable size ratio for enabling collection.

Regarding the effects of strength on the attenuation performance, the trends in Figure 5 suggest that the flocs with the greatest strength scale (20 ppm set) have the lowest collection capacity. When one considers the effect of polymers to boost strength, these will affect both the feed flocs and the flocs within the blanket, there being ample justification for believing that both would increase in size. If both were to increase in the same proportion, it would make no difference to the trapping efficiency as defined by Equation (48). What matters is the relative size; the collection efficiency improves when the sizes of the feed flocs and collector flocs become more comparable. In addition, one must consider the impact of changing strength on Φ_F.

CONCLUDING REMARKS

Insofar as one can judge, the framework described appears to accommodate the various strands of experimental evidence that have been presented. This task is made difficult by the lack of supporting information (e.g. A', S_o and D) for inclusion in the theory. Where 'guesstimates'

have been included, they appear to be satisfactory. The assumption of treating flocs as non-porous appears to have been satisfactory in the context of the analysis associated with Figure 2. One outcome of the theory is that it identifies critical parameters that affect the dynamics, which has benefits for experimental design.

The impacts of strength are complex. An immediate impact of increasing strength is to enable the development of larger and/or more compact feed flocs. However in the context of the blanket, the effects of strength are subtle, the outcome depending on the character of the particular floc. Increased strength does not necessarily enhance the mass flux, much depending on the magnitude of D. The observations of Gregory (1979) show that greater strength offers the prospect of attaining a greater value of Φ_F, a necessary feature for assuring attenuation. Theory suggests that the magnitude of the upflow goes hand in hand with the strength scale as suggested in Bache & Gregory (2007, Table 3.14).

There appears to be a case for aiming to achieve a blanket with as small a floc size as practicable in order to: promote the capture of feed flocs by interception; reduce the water content of the solids waste stream when using hydrolysing coagulants; and also enhance the mass flux.

There are aspects of the theory that warrant further scrutiny, but generally it provides a framework that can be developed further. Hopefully, the paper will stimulate thinking about the many issues involved.

ACKNOWLEDGEMENTS

The author gratefully acknowledges the many helpful comments provided by Ross Gregory during the preparation of this paper.

REFERENCES

Armirtharajah, A. & O'Melia, C. R. 1990 Coagulation processes: destabilisation, mixing and flocculation. *Water Quality and Treatment*, 4th edition. AWWA, McGraw Hill, pp. 269–365.

Bache, D. H. 2004 Floc rupture and turbulence: a framework for analysis. *Chem. Eng. Sci.* **59**, 2521–2534.

Bache, D. H. & Gregory, R. 2007 *Flocs in Water Treatment*. IWA Publishing, London.

Bache, D. H. & Rasool, E. 2006 Characterisation, scaling and analysis of steady state floc size distribution using a mass balance approach. *J. Water Supply: Res. Technol. AQUA* **55**(5), 335–356.

Bache, D. H., Rasool, E., Moffat, D. & Johnson, M. 2000 Floc characterisation at full scale: the case of humic waters. In: Hahn, H. H., Hoffman, E. & Ødegaard, H. (eds) *Chemical Water and Wastewater Treatment VI*. Springer, Heidelberg, pp. 66–76.

Furrer, F., Ludwig, C. & Schindler, P. W. 1992 On the chemistry of Keggin Al_{13} polymer. *J. Colloid Interface Sci.* **149**(1), 56–67.

Gmachowski, L. 2002 Hydrodynamic behaviour of suspensions. *Encyclopedia of Surface and Colloid Science*. Marcel Dekker, New York, pp. 2364–2374.

Gregory, R. 1979 *Floc Blanket Clarification*, Report TR111. WRc, Swindon, UK.

Gregory, R., Head, R. J. M. & Graham, N. J. D. 1996 The relevance of blanket solids concentration in understanding the performance of floc blanket clarifiers in water treatment. In: Hahn, H. H., Hoffmann, E. & Odegaard, H. (eds) *Chemical Water and Wastewater Treatment IV*. Springer, Heidelberg, pp. 17–29.

Gregory, R., Zabel, T. F. & Edzwald, J. K. 1999 Sedimentation and flotation. In: Letterman, R. D. (ed.) *Water Quality and Treatment: A Handbook of Community Water Supplies*, 5th edtion. AWWA, McGraw-Hill, New York.

Ives, K. J. 1968 Theory of operation of sludge blanket clarifier. *Proc. Inst. Civil Eng.* **39**, 243–260.

Probstein, R. F. 1994 *Physicochemical Hydrodynamics*, 2nd edition. Wiley-Interscience, New York.

Sonntag, R. C. & Russel, W. B. 1987 Structure and breakup of flocs subjected to fluid stresses. II. Theory. *J. Colloid Interface Sci.* **115**(2), 378–389.

Spielman, L. A. 1977 Particle capture from low-speed laminar flows. *Annu. Rev. Fluid Mech.* **9**, 297–319.

Su, S. T., Wu, R. M. & Lee, D. J. 2004 Blanket dynamics in upflow suspended bed. *Water Res.* **38**, 89–96.

Sung, S. S. & Lee, D. J. 2005 Huang Chihpin Steady state humic-acid-containing blanket in upflow suspended bed. *Water Res.* **39**, 831–838.

Tambo, N. & Hozumi, H. 1979 Physical aspect of flocculation process–II. Contact flocculation. *Water Res.* **13**, 421–448.

Tambo, N. & Watanabe, Y. 1979 Physical characteristics of flocs–I. The floc density function and aluminium floc. *Water Res.* **17**, 409–419.

Van Benschoten, J. E. & Edzwald, J. K. 1990 Chemical aspects of coagulation using aluminium salts–1. Hydrolytic reactions of alum and polyaluminium chloride. *Water Res.* **24**, 1519–1526.

First received 27 March 2009; accepted in revised form 13 October 2009